PHILOSOPHICAL TRANSACTIONS OF THE ROYAL SOCIETY A MATHEMATICAL, PHYSICAL & ENGINEERING SCIENCES

Ultracold collisions for Bose––Einstein condensation

L. S. Butcher, D. N. Stacey, C. J. Foot and K. Burnett

Phil. Trans. R. Soc. Lond. A 1999 **357**, 1421-1439
doi: 10.1098/rsta.1999.0382

THE ROYAL SOCIETY

Ultracold collisions for Bose–Einstein condensation

By L. S. Butcher†, D. N. Stacey, C. J. Foot and K. Burnett

Clarendon Laboratory, Department of Physics, University of Oxford, Parks Road, Oxford OX1 3PU, UK

We describe the low-energy scattering theory relevant to the description of the Bose–Einstein condensed gases recently produced using evaporative cooling. We examine the validity range of the approximations being used to describe the ultracold interactions in the context of the interaction between caesium atoms at the temperatures produced by evaporation in a magnetic trap. We discuss the prospects for future developments in the field.

Keywords: laser cooling; evaporative cooling; Bose–Einstein condensation; ultracold collisions; scattering length

1. Introduction

In July 1995, Anderson *et al*. (1995) reported the observation of Bose–Einstein condensation (BEC) in a gas of rubidium-87 atoms that had been trapped in a magnetic field and cooled to 170 nK. BEC occurs when the thermal de Broglie wavelength of the atoms is larger than their separation and leads to a rapid increase in the population of the lowest translational state available to the atoms. In the experiments at JILA this was the ground vibrational state of the magnetic trap in which the atoms were held. The exceptionally low temperatures required were reached using a combination of laser and evaporative cooling (Burnett 1996) and the build-up of atoms in the ground state was observed via the greatly enhanced density of atoms that it produced in the trap centre. The alkali gases used are so dilute that the interactions between the atoms do not appreciably alter the condensation process from that one would expect to see in an ideal gas. Once a condensate is formed, however, the interactions do affect the macroscopic properties that can be studied, e.g. collective modes. The interactions between alkali atoms can still be described in terms of binary ultracold collisions, and that is the subject we shall address in this article. (Condensate lifetimes are also limited by three-body recombination but we will only be able to take a cursory look at this process.) Although many aspects of BEC have previously been studied in relation to superconductivity and superfluidity, the evaporative cooling experiments were the first observation of the phenomenon in a dilute atomic gas. Other reports of BEC in lithium-7 and sodium quickly followed (Bradley *et al.* 1995; Davis *et al.* 1995). Since then, several other experimental groups have produced condensates in rubidium and sodium.‡ Alkali gases have turned out

† Present address: Pilkington Technology Management, Hall Lane, Lathom, Ormskirk, Lancashire L40 5UF, UK.

‡ For up-to-date information on BEC experiments and theory, one can consult the BEC Web site maintained by Mark Edwards at Georgia Southern University (amo.phy.gasou.edu/bec.html/).

to be the best systems for achieving BEC because of the possibility of cooling them to microkelvin temperatures using laser cooling. At these very low temperatures, they can be trapped in modest magnetic fields and cooled using evaporation. BEC is reached at such low temperatures (i.e. where the atoms have such large de Broglie wavelengths) that the density required is very low: typically below 10^{14} cm^{-3}. Other BEC experiments have used spin-polarized hydrogen, where the method of evaporative cooling was first developed for trapped atoms. This subject is reviewed by Walraven (1995). BEC has recently been achieved in hydrogen by Fried *et al.* (1998) at MIT.

In this article we shall discuss aspects of collision physics relevant to the description of BEC observed in the alkalis. We shall discuss what aspects of low-energy collision physics are relevant to the description of condensates and briefly outline our present state of knowledge of them. This will include studies we have made of the validity of low-energy approximations that have been used to date. We shall then turn to the methods by which information on the interatomic potential relevant to the ultracold collisions can be obtained, including our own work which involves high-resolution molecular spectroscopy. The ultracold collision processes that one has to study are providing a strong stimulus to the development of quantal collision theory that can treat fully the complexities of multichannel systems. We shall focus on the case of caesium to illustrate some of the complexities involved in studying the low-temperature scattering involved in these studies. Caesium is of particular interest as it is the element used in atomic clocks; the second being defined in terms of the frequency of a hyperfine transition in caesium. Many experiments on laser cooling and trapping of caesium have taken place in Oxford, Paris and elsewhere (Adams & Riis 1997). Caesium atoms have also been evaporatively cooled but Bose–Einstein condensation has not yet (as of April 1999) been observed in caesium. One of the reasons for the difficulty of obtaining BEC in Cs is the lack of information on the potential curves involved. This was the motivation for the work at Oxford on the molecular spectroscopy of the caesium molecule. Before discussing the details, we shall describe general aspects of the low-temperature collision physics which affects BEC.

2. Collisions and the condensate

The behaviour of atoms in collisions at low temperatures can be represented in many cases by a single parameter, the *scattering length*, α, if one can assume that only a single channel is involved. Unlike the radius of an equivalent hard sphere, the scattering length can have either positive or negative sign. A positive scattering length corresponds to effectively repulsive interactions, and a negative scattering length to effectively attractive interactions. The alkali gas condensates are dilute in the sense that the scattering length is much (typically a thousand times) smaller than the interparticle distance. This justifies the use of 'first principles' approaches to the theory of the condensates based on the theory of the dilute Bose gas (Huang 1963). Once one has a reliable determination of the scattering length one can proceed in confidence with calculations of the macroscopic properties of the condensates such as collective excitations. To see how this can be done in principle we shall discuss how the scattering length enters into the description of the condensate. The energy

of condensed atoms due to the presence of others is given by

$$n(\boldsymbol{r},t)U_0. \tag{2.1}$$

Here, U_0 depends on the scattering length α, thus

$$U_0 = h^2\alpha/2\pi m, \tag{2.2}$$

and the density $n(\boldsymbol{r},t) = |\Psi(\boldsymbol{r},t)|^2$ is given by the wave function shared by all the atoms in the condensate. The evolution of the condensate is described by a nonlinear Schrödinger equation called the Gross–Pitaevskii equation. In free space this has the form:

$$\mathrm{i}\hbar\frac{\partial\Psi}{\partial t} = -\frac{\hbar^2\nabla^2\Psi}{2m} + U_0|\Psi|^2\Psi. \tag{2.3}$$

For small k excitations this leads to the dispersion relation for longitudinal excitations in the condensate,

$$\omega = \sqrt{\frac{nU_0}{m}}k = ck. \tag{2.4}$$

This gives the speed, c, of longitudinal sound waves in the condensate. Since the sign of U_0 is the same as that of α (equation (2.2)), this suggests that only a positive scattering length will lead to a stable condensate, as a negative scattering length will lead to complex, i.e. unstable excitations. A condensate has been reported in lithium-7 (Bradley *et al.* 1995), which is known to have a negative scattering length (Abraham *et al.* 1995). In a trap the collapse of the condensate can be held off by the zero-point energy in the confined gas. Attractive forces between the atoms still makes the density in the condensate increase as atoms are added to it and for sufficiently large numbers collapse should occur. Evidence for this collapse has also been reported for lithium.

The fact that only longitudinal waves are supported by the gas means that it is a superfluid with a critical velocity c that depends only on the density (and mass) of the gas and the scattering length. The precise nature of the superfluidity that can be observed in trapped gases is still a matter of detailed investigations currently underway.

Cold collisions also determine the rate of evaporative cooling in the technique used to reach the very low temperatures required for Bose–Einstein condensation. In this technique, the depth of the magnetic trap holding the atom is decreased, so that faster atoms escape from the trap, leaving behind the cooler atoms (Ketterle & Van Druten 1996). For evaporative cooling to be effective, many elastic two-body collisions are required to maintain thermal equilibrium in the gas. It is the ratio of these 'good' elastic collisions to 'bad' or inelastic collisions that determines whether BEC can be obtained. For sodium and rubidium we know that this ratio is favourable; for caesium we are still uncertain. Three-body recombination also sets in at higher densities and produces loss of atoms from a trap. The latter process provides a formidable challenge to the molecular theorist. A recent advance in the theory of these three-body encounters has been used to show that the three-body recombination rate scales with α^4 (Fedichev *et al.* 1996*b*) in the low-temperature limit (in the case where the diatomic molecular state produced is weakly bound with zero orbital angular momentum).

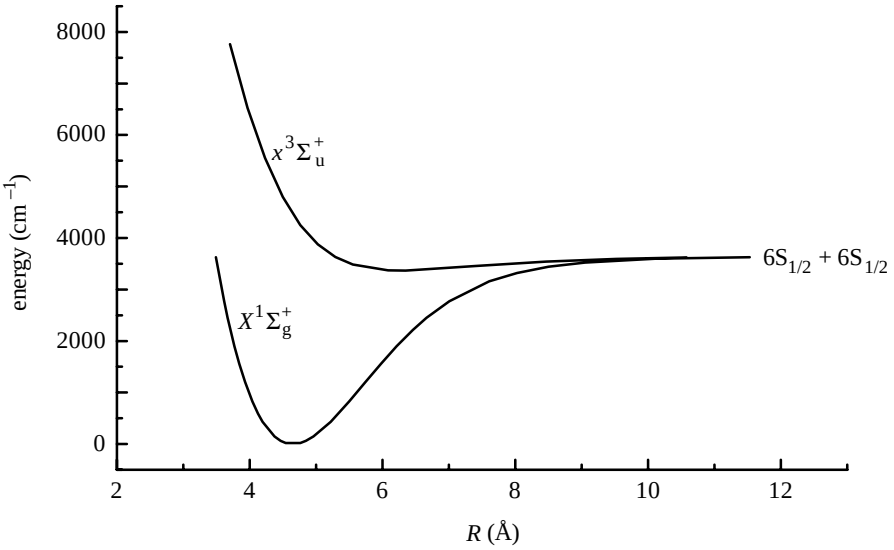

Figure 1. Ground state potentials for the Cs_2 molecule.

The study of cold collisions is also important in other areas. In atomic fountains for use as frequency standards (Gibble & Chu 1993), collisions between atoms perturb the atomic energy levels, and lead to frequency shifts of a few millihertz. Cold collisions have an effect in atom interferometry, where interactions give an effective 'refractive index' for the matter waves (Audouard *et al.* 1995). In the next section we shall discuss how the scattering length can be measured using a variety of techniques. Collisional and three-body recombination loss rates are so low that they have to be measured *in situ*, i.e. when performing evaporative cooling or observing the decay of condensed atoms.

3. Scattering lengths for the alkalis

There are several methods by which scattering lengths that we require to model BEC can be found. One way is to measure scattering lengths by studying processes that depend on them, for example the relaxation time of atoms in a magnetic trap (Arndt *et al.* 1997; Arlt *et al.* 1998) or frequency shifts in an atomic fountain (Verhaar *et al.* 1993). The intensities of transitions studied by photoassociation spectroscopy (Thorsheim *et al.* 1987) can be used to deduce the structure of the long-range molecular wave function and hence the scattering length (a more detailed description of photoassociation spectroscopy is given below). Photoassociation, when feasible, has provided by far the most detailed information on the relevant potentials.

The scattering length can, of course, be derived directly from the interatomic potential. This raises the question of how to determine the interatomic potential and we shall address this issue below. First we shall discuss the general features of the potentials that go to making the theory so complex and interesting. The ground-state interatomic potentials of Cs_2 are shown in figure 1.

At large separations the energies are clearly those of the free atoms (the *dissociation limit*). As the atoms come closer together, there are attractive forces between them. At very small separations the forces between the atoms are repulsive, and the

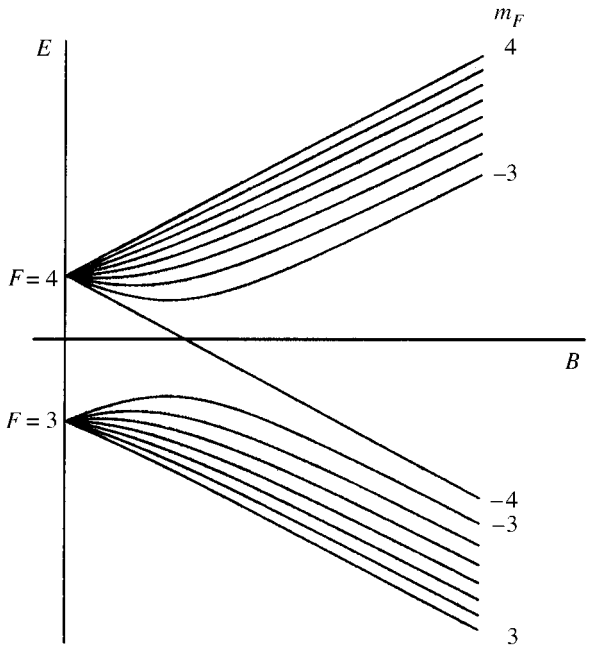

Figure 2. Cs hyperfine structure.

corresponding energy becomes large and positive. In the intermediate region there is an attractive potential well, which may give rise to discrete bound states. Figure 1 shows that there are in fact two different interatomic potentials corresponding to the total electronic spin $S = 0$ and $S = 1$ in these singlet and triplet states.

As the singlet and triplet ground states have different interatomic potentials, they also give rise to different scattering lengths α_{S} and α_{T}. The scattering states formed by the two atoms involved in the collision depend, due to the hyperfine interaction, not only on the alignment of the electronic spins, but also those of the nuclei. This means we cannot describe the states simply in terms of singlets and triplets. At intermediate separations the hyperfine and exchange interactions are comparable and one has in general to handle the molecular Hamiltonian in all its complexity as has been done by, for example, Leo *et al*. (1998). At large internuclear separations, the states tend, of course, to the atomic hyperfine states of definite F. For the case of elastic collisions between doubly polarized atoms, i.e. both atoms in the level $M_F = F$, the scattering is determined by the triplet potential. This is the case we shall use to illustrate the sensitivity of the scattering process to the precise form of the potential.

The hyperfine structure of the caesium atom as a function of applied magnetic field is shown in figure 2.

We are interested particularly in the states of the atoms that are amenable to trapping in an inhomogeneous magnetic field, as these are the ones that can be cooled using evaporation. Trapping in the fields available in the laboratory requires a low-field seeking hyperfine state (Tiesinga *et al.* 1992). There are two such states for caesium as shown in figure 2: the $(F, M_F) = (4, +4)$ and $(F, M_F) = (3, -3)$ states. The scattering length of the $(4, +4)$ state is given purely by α_{T}, while the scattering length which applies to the $(3, -3)$ state is a mixture of α_{T} and α_{S}. As the

Table 1. *Scattering lengths of the alkalis*

	α_S (a_0)	α_T (a_0)	techniques used	reference
^{6}Li	45.5 ± 2.5	-2160 ± 250	photoassociation spectroscopy	Abraham *et al.* (1997)
^{7}Li	33 ± 2	-27.6 ± 0.5	photoassociation spectroscopy	Abraham *et al.* (1997)
^{23}Na	34.9	77.3	molecular spectroscopy plus theoretical long- and short-range potential	Côté & Dalgarno (1994)
^{87}Rb		$+99 \rightarrow +119$	photoassociation spectroscopy	Boesten *et al.* (1997)
^{85}Rb		$-1200 \rightarrow -80$	photoassociation spectroscopy	Gardner *et al.* (1995)
^{133}Cs		$-200 \rightarrow -1100$	frequency shifts in atomic fountain	Verhaar *et al.* (1993)
		-250	theoretical potential	Pillet *et al.* (1997)

combination of the two scattering lengths is dependent on the applied magnetic field strength, the scattering length for the $(3, -3)$ state may be tunable with magnetic field (Tiesinga *et al.* 1992). Such tuning has been achieved in sodium by the MIT group (Inouye *et al.* 1998). It may also be possible to tune the scattering length using nearly resonant light (Fedichev *et al.* 1996*a*). This brief discussion shows that whichever hyperfine state is used, a knowledge of the triplet scattering length is valuable. However, the triplet scattering length in caesium is poorly known compared with the scattering lengths of the other alkalis. Table 1 shows some calculated values of scattering lengths for the alkali metals.

4. Calculation of scattering lengths

In this section we shall look at the sensitivity of scattering lengths to the form of interatomic potentials and give an assessment of the approximations commonly used. We shall not discuss the complex issues raised by the multichannel aspects of the collision process as these have been studied in detail by the NIST theory group (Leo *et al.* 1998).

If the potential does not support bound states, then finding the sign of the scattering length is straightforward; a purely repulsive potential leads to repulsive collisions, and a positive scattering length, while an attractive potential which supports no bound states leads to attractive collisions, and a negative scattering length. Where the potential supports bound states, however, the situation is more complex. The magnitude and sign of the scattering length depend critically on the exact shape of the potential, and in particular on the energy of the least-bound state. Hence a very accurate knowledge of the interatomic potentials is required to calculate the scattering length. As an example, we will apply our analysis to the case of the ground-state triplet potential of caesium.

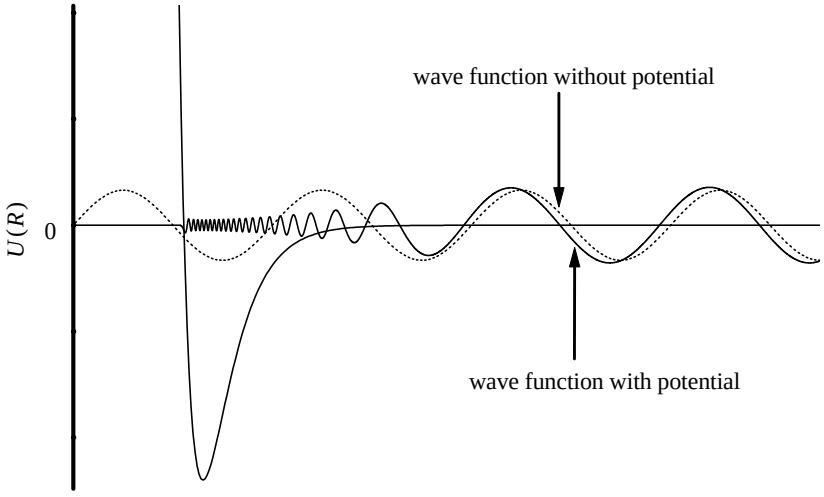

Figure 3. Typical partial wave.

(*a*) *Low-energy partial wave analysis*

In this section we give a brief review of the low-energy scattering theory that is relevant to the calculation of scattering lengths. It will also enable us to examine the limitations to a description of low-energy collisions in terms of the scattering length alone. Let us suppose that this potential is available to us from some method or other. Since the incoming particles have a small positive energy, the scattering states of the potential required will be equivalent to unbound molecular states, i.e. above the dissociation limit of the pair. To obtain the scattering state we solve for each partial wave that has the asymptotic form,

$$\chi_{\mathrm{l}}(R) = \sin(kR + \delta_{\mathrm{l}}(k)). \tag{4.1}$$

Here, δ_{l} is the phase shift introduced by the potential, and k is the wave vector $\hbar k = \sqrt{2mE}$. A typical example of such a partial wave is shown in figure 3.

All the information necessary to calculate the scattered wave function is, of course, contained in the phase shifts $\delta_{\mathrm{l}}(k)$ and the cross-section σ is given by

$$\sigma = \frac{4\pi}{k^2}\sum_{l=0}^{\infty}(2l+1)\sin^2\delta_{\mathrm{l}}. \tag{4.2}$$

If k is sufficiently small as it is in the case of the very low temperatures reached in evaporative cooling, then only the $l = 0$ term is important. In this approximation, we have *s-wave scattering*. For s-wave scattering, the total cross-section is given by

$$\sigma = \frac{4\pi\sin^2\delta_0(k)}{k^2} \tag{4.3}$$

and the scattering is isotropic.

For the simple case of a hard sphere the effect of the potential on the wave function is simply a shift in the origin of oscillations of the wave. The new wave function is then

$$\chi = \sin k(R-a). \tag{4.4}$$

The phase shift introduced by the potential is $-ka$, and so the cross-section for the hard sphere potential is simply

$$\sigma = 4\pi a^2. \tag{4.5}$$

Note that for the hard sphere, the cross-section is independent of the energy of the scattered particle. For a real potential this is only true of the extreme low-energy limit as we shall see below. A typical unbound wave function for such a potential is shown in figure 3. In contrast to the hard sphere case, the phase shift now depends on the energy, and hence wave vector, of the state. The phase shift also depends sensitively on the precise shape of the potential, as there are many fast oscillations of the wave function in the region of the potential well. If we wish to know the cross-section for a particular energy, we now need to calculate the phase shift for that particular energy, which rather reduces the elegance of the method. However, as we are interested in the low-temperature limit, we can consider only the phase shift as the energy tends to zero. If the phase shift remains small (we examine this approximation in a moment), then $\sin(\delta_0(k)) \sim \delta_0(k)$, and equation (4.3) becomes

$$\sigma = \frac{4\pi\delta_0(k)^2}{k^2}. \tag{4.6}$$

We define the scattering length in terms of the phase shift as the energy tends to zero:

$$\alpha = -\lim_{k\to 0} \frac{\delta_0(k)}{k}. \tag{4.7}$$

Using this definition in equation (4.6) then gives

$$\sigma = 4\pi\alpha^2. \tag{4.8}$$

Comparing this to the cross-section for a hard sphere in equation (4.5), we see that the cross-section for an arbitrary potential at zero energy is the same as that of a hard sphere with radius α. In the case where the phase shifts are small, $\delta_0(k)/k$ is roughly constant for small k. Hence the cross-section is given by equation (4.8) not only at $k = 0$, but also for small non-zero values of k. Just how large k can be is the matter we shall now address.

Figure 4 shows the wave function as the energy tends to zero. The wavelength tends to infinity, and so the wave function is effectively a straight line for large r. The intercept of this line, projected back to the x-axis, is the scattering length α.

(*b*) *The effect of bound states of the potential on* α

We shall now look more closely at how the phase shift is determined by the inner part of the potential, and particularly at the significance of the bound states.

There is a finite number of bound energy levels for ground-state interatomic potentials (Gribakin & Flambaum 1993), and hence a 'least-bound' level with energy $-\epsilon$ ($\epsilon > 0$). The scattering length depends critically on the position of this least-bound state, relative to the separated atoms (Landau & Lifshitz 1991). If ϵ is sufficiently large and the last bound state is not close to the top of the potential, then the phase shifts $\delta_0(k)$ remain small, and we have the wave function shown in figure 5*a*. If we make a small change in the potential so that ϵ becomes larger, the least-bound state moves away from the dissociation limit, and the scattering length decreases. A

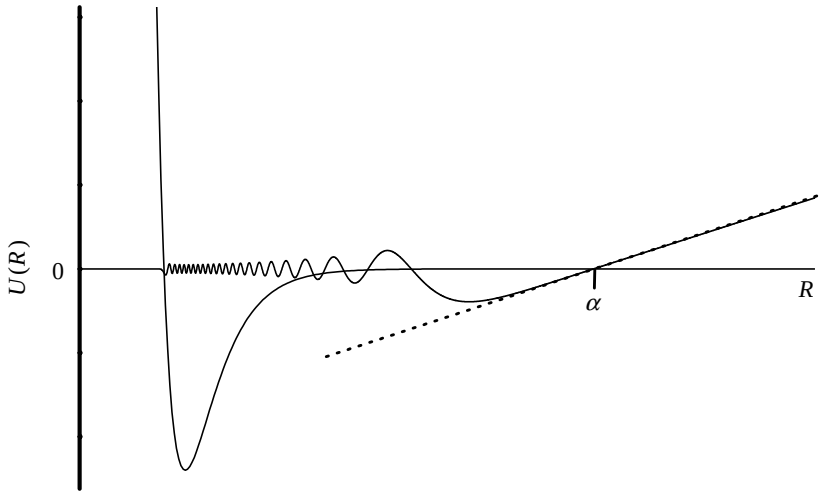

Figure 4. Wave function for low energy, showing the scattering length.

further change will result in a 'virtual level' approaching the dissociation limit from above. Just before this state becomes bound, the scattering length is very large and negative (figure 5*b*). As the state becomes bound, the wave function 'turns over', as one extra bound state means one more node in the wave function, and the scattering length becomes large and positive (figure 5*c*).

We see that the scattering length depends very sensitively on the position of the least-bound state, especially when this state is close to the dissociation limit. In the case where the least-bound state is very close to the dissociation limit, or if there is a 'virtual' nearly bound level (i.e. if ϵ is small), the energy of the scattered particle, E, is almost 'in resonance' with the level $-\epsilon$, which leads to a significant increase in the phase shifts and cross-section. In this *resonance scattering* case, equation (4.8) no longer applies (Landau & Lifshitz 1991). The cross-section in the case where there is a weakly bound level can be found by considering Schrödinger's equation for large and small R, and then considering the boundary condition that the two solutions match (Landau & Lifshitz 1991) to give

$$\sigma = \frac{2\pi\hbar}{\mu(E+\epsilon)}, \tag{4.9}$$

where E is the energy of the scattered particle above the dissociation limit.

(i) *The effective range expansion*

We now have two different expressions for the cross-section, valid in opposite regimes. It is possible, however, to find an expression from equation (4.3) which is valid in both cases, by using the well-known *effective range expansion*. The phase shift can be written as a power-series expansion in k:

$$k\cot\delta_0(k) = -\frac{1}{\alpha} + \tfrac{1}{2}r_0k^2 + O(k^3), \tag{4.10}$$

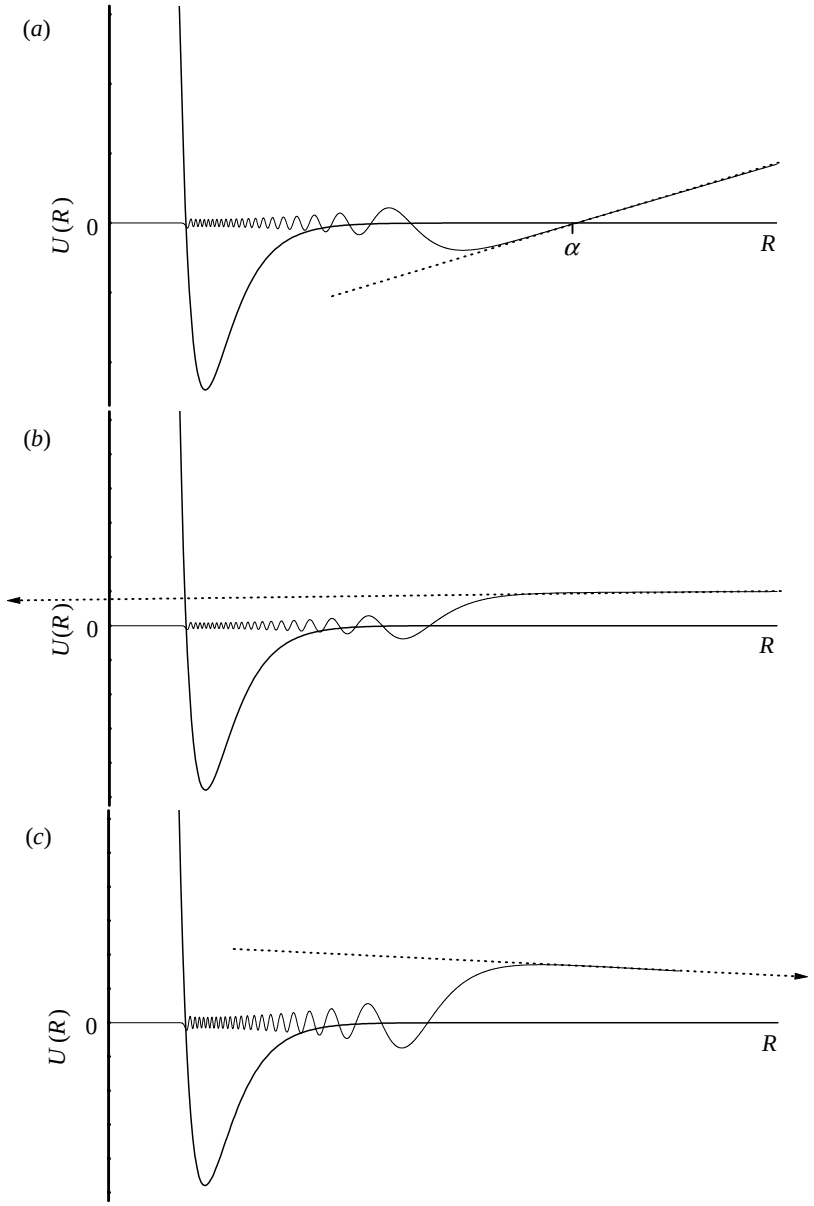

Figure 5. The wave function for three different cases as described in the text.

where r_0 is the *effective range*. Substituting equation (4.10) into (4.3), and keeping terms up to k^2 gives (Mott & Massey 1965)

$$\sigma = \frac{4\pi\alpha^2}{k^2\alpha^2 + (1 - r_0 k^2 \alpha)}. \tag{4.11}$$

In the limit of low energies or small $|\alpha|$ this reduces to the scattering length form of equation (4.8). This expression is also valid when there is a bound state near the dissociation limit. For a bound state with energy $|E| = \hbar^2\kappa^2/2\mu$, α and r_0 are related

by

$$-\frac{1}{\alpha} = -\kappa + \tfrac{1}{2} r_0 \kappa^2. \tag{4.12}$$

This form for the cross-section has the advantage that it is applicable across a wide range of scattering lengths (Leo *et al.* 1998).

(ii) *Validity of approximate expressions for the cross-section*

We now have four formulae for the s-wave cross-section, which are predicted to be valid in different circumstances:

$$\sigma = \frac{4\pi \sin^2 \delta_0(k)}{k^2} \qquad \text{(exact)}, \tag{4.13 a}$$

which is valid for all δ_0;

$$\sigma = \frac{4\pi\alpha^2}{k^2\alpha^2 + (1 - r_0 k^2 \alpha)} \qquad \text{(effective range)}, \tag{4.13 b}$$

which is valid for reasonably low k, all α;

$$\sigma = 4\pi\alpha^2, \qquad \alpha = -\lim_{k\to 0} \frac{\delta_0}{k} \qquad \text{(scattering length)}, \tag{4.13 c}$$

which is valid for small δ_0, which is the case when the least-bound state ϵ is sufficiently far from the top of the potential;

$$\sigma = \frac{2\pi\hbar^2}{\mu(E + \epsilon)} \qquad \text{(resonance)}, \tag{4.13 d}$$

which is valid when the least-bound state is close to the top of the potential.

However, it is not immediately obvious for what values of ϵ (4.13 *b*)–(4.13 *d*) will be good approximations. The validity of each approximation may also depend on k; (4.13 *c*) will always be true for $k = 0$ by definition, but will become an increasingly worse approximation for large k.

We have investigated the conditions under which the approximations hold by calculating the phase shifts numerically, using a potential similar to the expected form of the caesium ground-state triplet potential. For this we use a Morse potential:

$$U(R) = D_\mathrm{e}\{1 - \mathrm{e}^{-\beta(R - R_\mathrm{e})}\}, \tag{4.14}$$

where D_e is the dissociation energy, R_e is the equilibrium separation of the atoms, and β is a parameter giving the 'steepness' of the potential, derived from the rotational constant B_e. We use the theoretical parameters of the caesium triplet potential found by Speiss (1989):

$$D_\mathrm{e} = 240\ \mathrm{cm}^{-1}, \tag{4.15}$$

$$\omega = 11.2\ \mathrm{cm}^{-1}, \tag{4.16}$$

$$B_\mathrm{e} = 5.97 \times 10^{-3}\ \mathrm{cm}^{-1}, \tag{4.17}$$

which give the parameters for the Morse potential,

$$\beta = 0.720\ \text{Å}^{-1}, \tag{4.18}$$

$$R_\mathrm{e} = 6.496\ \text{Å}. \tag{4.19}$$

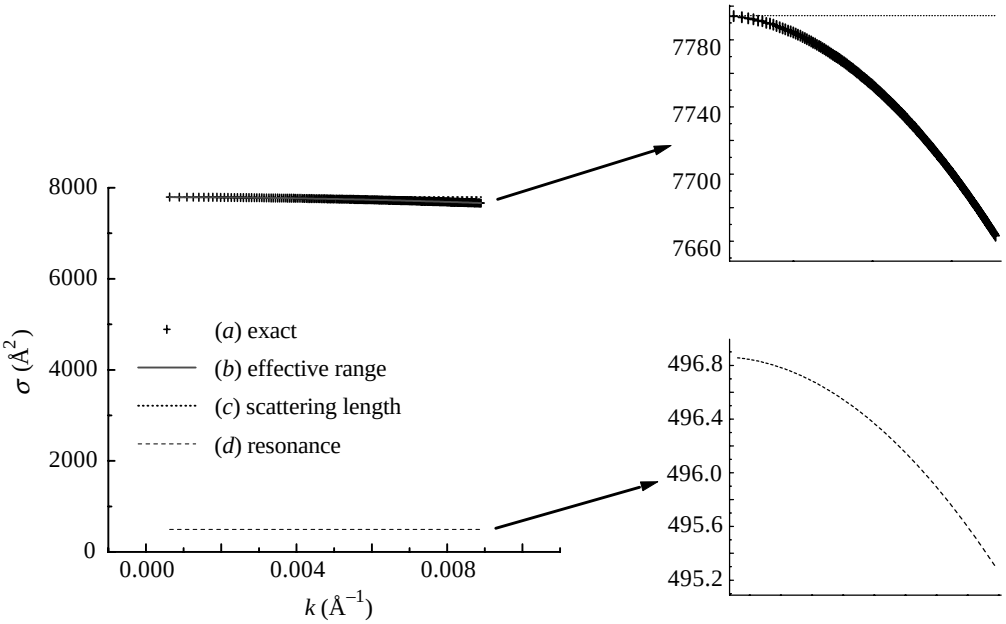

Figure 6. Cross-section against k for different approximations defined in the text. The graphs on the right give two expanded-scale versions of the main graph to display the slow variations not apparent in the summary plots.

We calculated the potential from $R = 0.008$ to 80 Å at intervals of 0.008 Å, and found values of δ_0 for particle energies from 10^{-7} cm^{-1} to 2×10^{-5} cm^{-1} (1 μK to 200 μK) for this potential. On plotting δ_0 against k for this potential, we found that the graph was a good approximation to a straight line. The scattering length is given by $-\delta_0/k$ as $k \to 0$. Since the gradient is almost constant, it suggests that the scattering length model is a good one in this case. To confirm this, we plotted values of σ against k as calculated from the general expression of (4.13 *a*), and compared this with the three models (4.13 *b*)–(4.13 *d*) (figure 6).

The values of σ found in the scattering length approximation (4.13 *b*) agree closely with the values found from (4.13 *a*), while those calculated using the resonance approximation (4.13 *c*) differ substantially. Hence, in this case, the scattering length model is the better one. We calculated the position of the highest bound state for this potential, and found it to be at 0.0064 cm^{-1} from the dissociation limit.

We then looked at the case when the last bound state is closer to the top of the well. We varied the parameter β in the Morse potential, and for each value calculated the phase shift for an energy of 10^{-7} cm^{-1}. Figure 7 shows the phase shift, the cross-section σ, and $\ln \sigma$ against β.

Arbitrary rotations of π in the phase are chosen to make the function continuous.

As β decreases, the last bound state moves closer to the dissociation limit, until the state is only just bound. This confirms the theory of § 4 *b*; when a state is just bound, the cross-section becomes very large, and the scattering length passes from large and positive to large and negative as the potential changes so that the state is no longer bound. We then chose the value of β to be 0.707 04 Å^{-1}, for which the state is just bound, and again calculated the phase shifts over the same range of

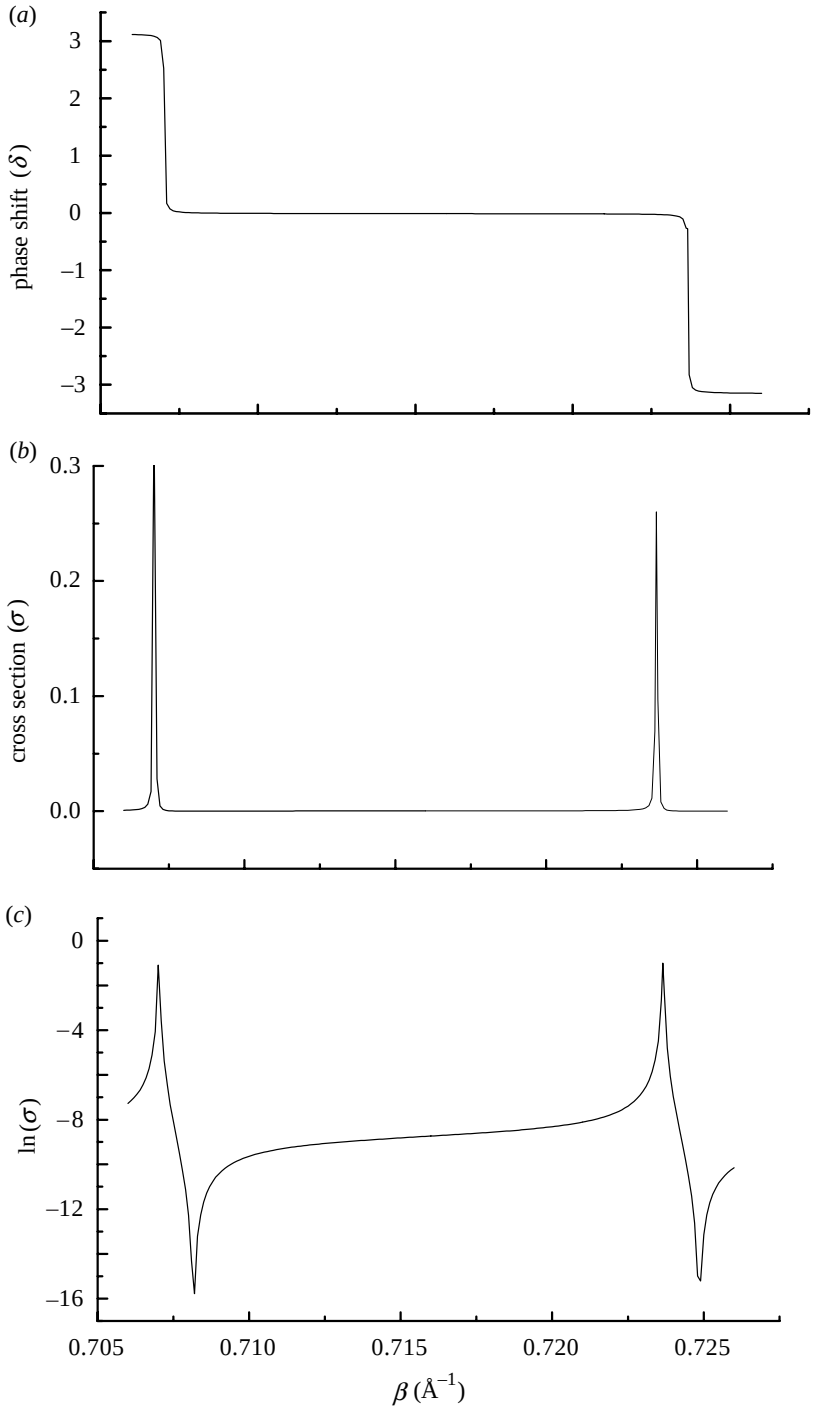

Figure 7. (*a*) Phase shift; (*b*) cross-section σ; (*c*) $\log(\sigma)$ against β.

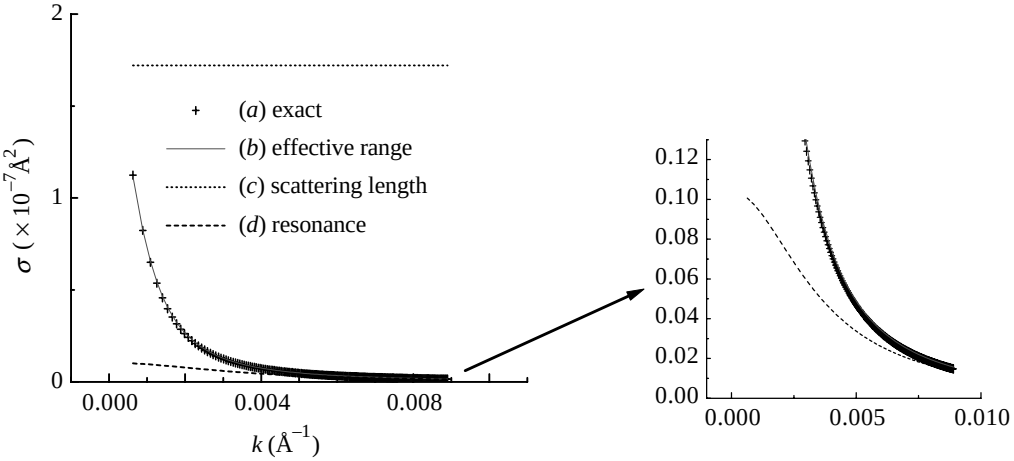

Figure 8. Cross-section against k for different approximations described in the text, close to a bound state.

energies. We plotted the cross-section calculated from (4.13 *a*), and compared the result with models (4.13 *b*)–(4.13 *d*), as shown in figure 8. In this case, the scattering length model is much worse, and the cross-sections approach those given by the resonance formula. However, the effective range formula still gives the best fit to the data.

From these calculations, we conclude that equation (4.8) is not a good approximation to the cross-section at any but the very lowest energies when there is a state which is very weakly bound. Since recent observations by Arndt *et al.* (1997) and Arlt *et al.* (1998) suggest that there is such a level for the caesium triplet ground state, we must look to a better approximation. The effective range expansion provides much better fits for the addition of only one extra parameter.

In our discussion so far we have restricted ourselves to a qualitative account of the variation of the scattering length. Because of its potential importance other detailed calculations have been undertaken by Leo *et al.* (1998). These calculations also included the effects of hyperfine structure on the collision complex although it does not have much influence on the elastic scattering. In these calculations the lack of sufficiently detailed information on the underlying potential meant they had to study the collisions for a range of potentials. They were not able, because of the remaining uncertainties, to rule out a large positive scattering length.

5. Methods for finding interatomic potentials

(*a*) *Ab initio methods*

We have shown how the scattering length depends critically on the exact shape of the interatomic potential, and in particular on the position of the last bound state. In this section, we will review briefly the methods used to derive interatomic potentials, discuss the progress to date, and the possibilities for the future.

One method is to use *ab initio* potentials for the short-range part of the potential (Krauss & Stevens 1990; Foucrault *et al.* 1992). These are not generally sufficient to be used alone except for the lightest alkalis, but are useful to supplement experi-

mental data. For the long-range part of the potential direct calculations play a more important role. The form of the attractive force between the atoms at long range is due to the Van der Waals, dipole–quadrupole, quadrupole–quadrupole, etc., interactions. These lead to a long-range potential of the form:

$$U(R) = -\frac{C_6}{R^6} - \frac{C_8}{R^8} - \frac{C_{10}}{R^{10}} \cdots . \tag{5.1}$$

Values of the constants $C_6, C_8, C_{10}, \ldots$ can be calculated theoretically (Marinescu & Dalgarno 1995; Marinescu *et al.* 1994), or found experimentally (see, for example, Weickenmeier *et al.* 1985). These long-range parameters complement experimental work, as experiments can often find only the short-range part of the potential. In a recent estimate of the caesium triplet scattering length, Pillet *et al.* (1997) used a theoretical potential and long-range parameters, finding a scattering length of $-250a_0$, which is within the range found by Verhaar *et al.* (1993) using experimental clock shifts. Leo *et al.* (1998) used *ab initio* potentials for the short range, whereas information on the medium-range singlet potential was obtained from experiment. Perturbation theory results were used for the for the long-range part of the potential. As mentioned above, this combination of sources does not tie the potentials down well enough to eliminate the uncertainties in the scattering length. This has been a continuing source of uncertainty in the analysis of evaporative cooling experiment in caesium.

(i) *Molecular spectroscopy*

An alternative method is to find the potentials experimentally using molecular spectroscopy, i.e. via the measurement of rovibrational structure in the relevant electronic states. These are the bound molecular states below the dissociation limit that separates them from the free molecular states that constitute the cold collision complexes that we have been discussing. The range of wavelengths needed for the relevant electronic transitions for the alkali molecules can be accessed by single-mode tunable lasers and high-resolution molecular spectra can therefore be produced.

The diatomic alkali molecules are rather unstable at room temperatures, but may be formed in a supersonic expansion, in which a vapour of the alkali metal, mixed with an inert carrier gas, is cooled by forcing it through a small nozzle into a vacuum. The gas cools in the expansion to temperatures of the order of a few kelvins, and under these conditions, molecules can form for long enough for spectra to be observed. In this technique, only the lowest states of the molecule are populated, and the absorption spectra are correspondingly simple. This aids the spectroscopic analysis but severely limits the access to information on the threshold region that is so important for cold collisions. This technique has been favoured for studying the triplet ground state of caesium (Kim & Yoshihara 1993; Diemer *et al.* 1991). We have studied caesium dimers using cold molecules formed in this way, probed with a tunable dye laser (Butcher *et al.* 1999), and measuring the total laser induced fluorescence; however, in common with previous work, we find that it is only possible to access the few very lowest vibrational levels of the ground state in this way. The analysis of the spectra is exceedingly complex due to the presence of hyperfine structure. In the lighter alkalis the availability of high-resolution spectra linked with the recent development of efficient multichannel computational methods has led to a very full understanding of the spectra, in spite of the complexities due to hyperfine

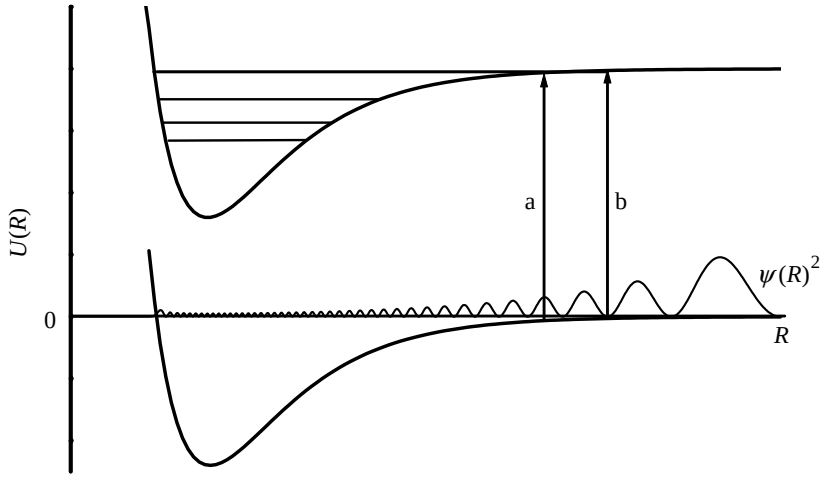

Figure 9. Transitions occurring in photoassociation spectroscopy. The variation in intensity gives information on the nodes of the wave function. In the figure, transition 'a' corresponds to peak and transition 'b' to a minimum in the intensity observed.

structure. It is to be hoped that a similar outcome is not too far in the future for caesium.

(ii) *Photoassociation spectroscopy*

An alternative and complementary technique, by which the highest lying levels of the ground state can be accessed, is that of photoassociation spectroscopy. Photoassociation spectroscopy was first proposed in 1987 by Thorsheim *et al.* (1987). In this technique alkali atoms are first confined in a magneto-optical trap or far off resonance optical dipole force trap (FORT). A pair of colliding ultracold atoms in the trap can resonantly absorb a laser photon to produce a bound, excited molecule. Photons are provided either by an additional laser, or by the FORT laser itself. As the laser is tuned, absorption peaks occur when the frequency corresponds to a transition between the dissociation limit of the ground state and a bound vibrational level of the excited state (see figure 9). The excited state molecules formed may then decay either to a bound ground-state molecule, or to an unbound atom pair (Abraham *et al.* 1996).

Either the fluorescence from the transition or the number of atoms in the trap can be monitored: the molecules which drop back to the ground state are lost from the trap. Normally we would expect to see only broad diffuse bands arising from free-bound transitions; but in the case of ultracold laser cooled atoms, the energy spread of the initial colliding atoms is very small (21 MHz at $T = 1$ mK). Hence the linewidth of these free-bound transitions will be comparable to that of bound–bound transitions; the technique is analogous to the laser-induced fluorescence (LIF) technique used in our experiments. The resulting spectrum gives the energy levels of the excited molecular state. In addition, information on the ground-state potential and scattering wave function can be obtained from line shapes and intensity distributions.

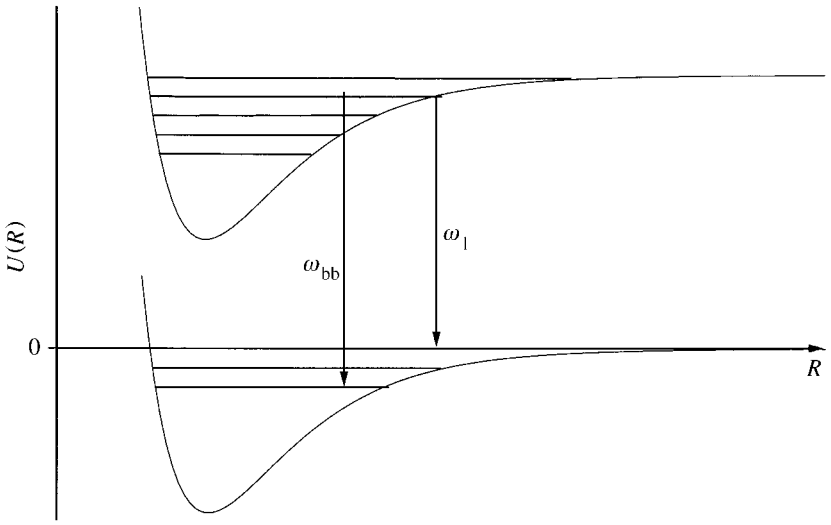

Figure 10. Transitions for two-photon photoassociation spectroscopy.

The technique can be extended to give information about the vibrational levels of the ground-state potential, not only the dissociation limit (Abraham *et al.* 1995). To do this the photoassociation laser frequency ω_l is fixed on a resonance, increasing the loss from the trap, and so decreasing the trap fluorescence. A second laser of frequency ω_{bb} is then used to tune over transitions between the excited state, and bound states of the ground-state potential. When this second laser is tuned to a resonance, the rate of loss from the trap is reduced, and the trap fluorescence increases (see figure 10).

Photoassociation spectroscopy has two major advantages over LIF. Firstly, as the initial state is formed in a collision, both singlet and triplet states can be studied. Secondly, it is the higher lying states needed to calculate scattering lengths which are excited; these cannot be studied easily using LIF.

However, photoassociation spectroscopy is difficult. Although it has been used successfully to study Li_2, Na_2 and Rb_2 and K_2, an attempt to observe photoassociation in caesium at NIST was unsuccessful; in Paris, Pillet *et al*. have now made preliminary observations. Caesium presents a particular problem as the photoassociation rate is predicted to decrease with increasing atomic mass from Li to Cs; observations of photoassociation in caesium by studying trap loss in an MOT are also made more difficult because the rate of trap loss due to photoassociation also decreases with increasing mass (Pillet *et al.* 1997).

6. Future work

The rapid expansion in the study of ultracold gases and condensates using evaporative cooling is likely to continue in the next decade. This means we shall have to understand and predict the outcome of nanokelvin collisions in magnetic and optical traps. We anticipate the need for interatomic potentials for mixed-species collisions in magnetic and laser fields. We should also be thinking about how we can perform experiments that give us a better handle on the three-body processes that limit the densities that can be reached in condensates. The atom we chose to study in Oxford has proven particularly intractable. In order to resolve the uncertainties

in the caesium interatomic potential, it appears it will be necessary to extend the present bound–bound spectroscopy to the use of Raman transitions that can access the high lying states of the ground triplet potential. Meanwhile, experiments planned in hybrid (magnetic plus optical trapping) may well resolve the question of whether BEC can be reached.

We thank the EPSRC for their support.

References

Abraham, E. R. I., McAlexander, W. I., Sackett, C. A. & Hulet, R. G. 1995 *Phys. Rev. Lett.* **78**, 1315.

Abraham, E. R. I., McAlexander, W. I., Gerton, J. M., Hulet, R. G., Côté, R. & Dalgarno, A. 1996 *Phys. Rev.* A **53**, R3713.

Abraham, E. R. I., McAlexander, W. I., Gerton, J. M., Hulet, R. G., Côté, R. & Dalgarno, A. 1997 *Phys. Rev.* A **55**, R3299.

Adams, C. S. & Riis, E. 1997 *Prog. Quant. Electr.* **21**, 1.

Anderson, M. H., Ensher, J. R., Matthews, M. R., Wieman, C. E. & Cornell, E. A. 1995 *Science* **269**, 198.

Arlt, J., Bance, P., Hopkins, S., Martin, J., Webster, S., Wilson, A., Zetie, K. & Foot, C. J. 1998 *J. Phys. Lett.* B **31**, 321–327.

Arndt, M., Ben Dahan, M., Guéry-Odelin, D., Reynolds, M. W. & Dalibard, J. 1997 *Phys. Rev. Lett.* **79**, 625.

Audouard, E., Duplàa, P. & Vigué, J. 1995 *Europhys. Lett.* **32**, 397.

Boesten, H. M. J. M., Tsai, C. C., Gardner, J. R., Heinzen, D. J. & Verhaar, B. J. 1997 *Phys. Rev.* A **55**, 636.

Bradley, C. C., Sackett, C. A., Tollett, J. J. & Hulet, G. G. 1995 *Phys. Rev. Lett.* **75**, 1687.

Burnett, K. 1996 *Contemp. Phys.* **77**, 1.

Butcher, L. S., Stacey, D. N. & Burnett, K. 1999 *J. Chem. Phys.* (Submitted.)

Côté, R. & Dalgarno, A. 1994 *Phys. Rev.* A **50**, 4827.

Davis, K. B., Mewes, M.-O., Andrews, M. R., Van Druten, N. J., Durfee, D. S., Kurn, D. M. & Ketterle, W. 1995 *Phys. Rev. Lett.* **75**, 3969.

Diemer, U., Gress, J. & Demtröder, W. 1991 *Chem. Phys. Lett.* **178**, 30.

Fedichev, P. O., Kagan, Y., Shlyapnikov, G. V. & Walraven, J. T. M. 1996*a* *Phys. Rev. Lett.* **77**, 2913.

Fedichev, P. O., Reynolds, M. W. & Shlyapnikov, G. V. 1996*b* *Phys. Rev. Lett.* **77**, 2921.

Foucrault, M., Millie, Ph. & Daudey, J. P. 1992 *J. Chem. Phys.* **96**, 1257.

Fried, D. G., Killian, T. C., Willmann, L., Landhuis, D., Moss, S. C., Kleppner, D. & Greytak, T. J. 1998 *Phys. Rev. Lett.* **81**, 3811.

Gardner, J. R., Cline, R. A., Miller, J. D., Heinzen, D. J., Boesten, H. M. J. M. & Verhaar, B. J. 1995 *Phys. Rev. Lett.* **74**, 3764.

Gibble, K. & Chu, S. 1993 *Phys. Rev. Lett.* **70**, 1771.

Gribakin, G. F. & Flambaum, V. V. 1993 *Phys. Rev.* A **48**, 546.

Huang, K. 1963 *Statistical mechanics*. New York: Wiley.

Inouye, S., Andrews, M. R., Stenger, J., Miesener, H.-J., Stamper-Kurn, D. M. & Ketterle, W. 1998 *Nature* **392**, 151.

Ketterle, W. & Van Druten, N. J. 1996 *Adv. At. Molec. Opt. Phys.* **37**, 181.

Kim, B. & Yoshihara, K. 1993 *Chem. Phys. Lett.* **204**, 407.

Krauss, M. & Stevens, W. J. 1990 *J. Chem. Phys.* **93**, 4236.

Landau, L. D. & Lifshitz, E. M. 1991 *Quantum mechanics*. Oxford: Pergamon.

Leo, P. J., Tiesinga, E., Julienne, P. S. & Walker, T. G. 1998 NIST preprint.
Marinescu, M. & Dalgarno, A. 1995 *Phys. Rev.* A **52**, 311.
Marinescu, M., Sadeghpour, H. R. & Dalgarno, A. 1994 *Phys. Rev.* A **49**, 982.
Mott, N. F. & Massey, H. S. W. 1965 *The theory of atomic collisions*. Oxford University Press.
Pillet, P., Crubellier, A., Bleton, A., Dulieu, O., Nosbaum, P., Mourachko, I. & Masnou-Seeuws, F. 1997 *J. Phys.* B **30**, 2801.
Spiess, N. 1989 PhD thesis, Fachbereich Chemie, Universität Kaiserslautern.
Thorsheim, H. R., Weiner, J. & Julienne, P. S. 1987 *Phys. Rev. Lett.* **58**, 2420.
Tiesinga, E., Moerdijk, A. J., Verhaar, B. V. & Stoof, H. T. C. 1992 *Phys. Rev.* A **46**, R1167.
Verhaar, B., Gibble, K. & Chu, S. 1993 *Phys. Rev.* A **48**, R3429.
Walraven, J. T. M. 1995 *Phys. World*, July, pp. 37–41.
Weickenmeier, W., Diemer, U., Wahl, M., Raab, M. & Demtröder, W. 1985 *J. Chem. Phys.* **82**, 5354.

PHILOSOPHICAL TRANSACTIONS OF THE ROYAL SOCIETY A MATHEMATICAL, PHYSICAL & ENGINEERING SCIENCES

PHILOSOPHICAL TRANSACTIONS OF THE ROYAL SOCIETY A MATHEMATICAL, PHYSICAL & ENGINEERING SCIENCES